

# Interfacial Microvoid Formation of Poly(vinyl chloride)/Polyacrylonitrile Blend Hollow-Fiber Membranes

Shuo Mei, Changfa Xiao, Xiaoyu Hu

State Key Laboratory of Hollow Fiber Membrane Materials and Process, Tianjin Polytechnic University, Tianjin 300160, China

Received 20 January 2011; accepted 21 April 2011

DOI 10.1002/app.35387

Published online 29 November 2011 in Wiley Online Library (wileyonlinelibrary.com).

**ABSTRACT:** Poly(vinyl chloride) (PVC)/polyacrylonitrile (PAN) blend hollow-fiber membranes were prepared by a phase-inversion method with water as inner and outer coagulations. The influence of the compatibility of the two polymers on the formation of interfacial microvoids (IFMs) in the PVC/PAN blend hollow-fiber membranes was investigated by the theory of thermodynamics and examined by Fourier transform infrared spectroscopy, dynamic mechanical analysis, viscometry, and scanning electron microscopy. All of the results show that good compatibility did not exist in the PVC/PAN blend sys-

tems; this led to the formation of IFMs between the two polymers. Also, the performance of the experimental results showed that the addition of PAN contributed to the enhancement of the permeability of the blend membranes; this laid the foundation for further study of PVC/PAN blend hollow-fiber membranes with antifouling properties after hydrolysis. © 2011 Wiley Periodicals, Inc. *J Appl Polym Sci* 124: E9–E16, 2012

**Key words:** immiscibility; interfaces; membranes; poly(vinyl chloride) (PVC)

## INTRODUCTION

Blending for polymeric membrane preparation is a useful method for obtaining novel membrane materials with special structure and new desirable properties and is also the least expensive, and it has also put much attention on the ultrafiltration, microfiltration, and pervaporation membrane fields.<sup>1–6</sup> As the most industrialized polymer, poly(vinyl chloride) (PVC) is fit for membrane materials, such as halogens, oxidants, inorganic acids, alkalis, and solvents, because of its mechanical performance, low cost, and excellent physical properties and chemical resistance.<sup>7</sup> However, the poor hydrophilicity of PVC remains a main problem and limits its wide application; thus, the hydrophilic modification of PVC membranes is one of the hotspots in membrane science. Several blend systems in PVC membranes, such as PVC/ethylene vinyl acetate (EVA), PVC/polyvinylidene fluoride (PVDF), PVC/chlorinated polyvinyl chloride (CPVC), PVC/polyvinylbutyral (PVB), PVC/polyacrylonitrile (PAN), and PVC/SiO<sub>2</sub>, have been investigated in the preparation of blend

membranes to improve the performance of PVC membranes.<sup>8–15</sup> PAN is a kind of polymeric material for making ultrafiltration membranes. It possesses good hydrophilicity and other advantages.<sup>16–18</sup> Some researches have indicated that ethanol exposure permanently alters the ultrastructural morphology and the transport properties of PAN/PVC hollow-fiber membranes.<sup>19</sup> Although the morphology of a PAN/PVC blend system has been studied, a compatible relationship between PVC and PAN, which introduces interfacial microvoids (IFMs) and subsequently affects the performance of the PVC/PAN blend hollow-fiber membranes, has rarely been reported.

In this study, PVC/PAN blend hollow-fiber membranes were prepared with the phase-inversion method. The compatibility between PVC and PAN was analyzed by the theory of thermodynamics and examined with dynamic mechanical analysis (DMA), Fourier transform infrared (FTIR) spectroscopy, viscosity measurements, and scanning electron microscopy (SEM). The effect of IFMs on the performance of the PVC/PAN blend hollow-fiber membranes was also studied.

Correspondence to: C. Xiao (xiaocf@yahoo.cn).

Contract grant sponsor: National Natural Science Foundation of China; contract grant number: 20874073.

Contract grant sponsor: Science and Technology Plans to Support Key Projects of Tianjin, China; contract grant number: 10SYSYJC27900.

*Journal of Applied Polymer Science*, Vol. 124, E9–E16 (2012)  
© 2011 Wiley Periodicals, Inc.

## EXPERIMENTAL

### Materials

PVC resins, whose average degrees of polymerization were 1000 and 1100, respectively, were purchased from Tianjin Dagu Chemical Plant (Tianjin, China). PAN (5000), kindly provided by Shandong Qilu

Petrochemical Engineering Co., Ltd. (Shandong, China), was dried for 24 h in a vacuum oven before use. *N,N*-dimethylacetamide (DMAC; >99%), from the Institute of Membrane Science and Technique, Tianjin Polytechnic University, was used without further purification.

### Preparation of the PVC/PAN blend hollow-fiber membranes

The PVC/PAN blend hollow-fiber membranes were prepared by the phase-inversion method. PVC and PAN were dried directly in a vacuum oven for approximately 20 h at 70°C to remove the water content. Then, dope blend spinning solutions were prepared from the dissolution of the polymer in DMAC at various ratios of PVC to PAN. The total polymer content was 17 wt %. With strong stirring for 12 h at 80°C, the resulting homogeneous solution was transferred to a stainless steel reservoir and was then degassed overnight at 60°C *in vacuo* to remove the bubble. After that, it was cast into a hollow fiber under a spinning apparatus; detailed spinning procedures were described elsewhere. In spinning, outer/inner diameters of the spinneret of 2500/1000 μm were used. The dope solution was extruded under a pressure of 0.3–0.4 MPa. Here, all of the ratios of dope solution rates and bore fluid rates were constant in the spinning processes. Water was used for internal and external coagulation baths. After the formation process, the PVC/PAN blend hollow-fiber membranes were stored in water for 2 days to remove solvents and were then immersed into a tank containing a 60% glycerol solution for 1 day and examined.

### Measurements

#### Viscosity method<sup>20</sup>

Viscosity measurements were made with an Ubbelohde dilution viscometer at 30.00 ± 0.02°C. The intrinsic viscosities were to zero concentration (*c*) according to Huggins [Eq. (1)] and Kraemer [Eq. (2)]:

$$\frac{\eta_{sp}}{c} = [\eta] + K_H[\eta]^2c \quad (1)$$

$$\frac{\ln \eta_r}{c} = [\eta] + K_K[\eta]^2c \quad (2)$$

where  $\eta_{sp}$  is the specific viscosity,  $\eta_r$  is the relative viscosity, and  $K_H$  and  $K_K$  are the Huggins and Kraemer constants, respectively.  $\eta_{sp}$  and  $\eta_r$  were determined from the following eqs. (3) and (4):

$$\eta_r = \frac{\eta}{\eta_0} = \frac{t}{t_0} \quad (3)$$

$$\eta_{sp} = \eta_r - 1 \quad (4)$$

where  $\eta_r$  and  $\eta_0$  are the viscosities of the polymer solution and the pure solvent, respectively, and  $t$

and  $t_0$  are the flow times of the polymer solution and pure solvent, respectively, through the Ubbelohde viscometer (h). The flux times were recorded with an accuracy of ±0.05 s. Extrapolation from the data obtained for five *c*s of the solutions was used to evaluate the intrinsic viscosity. From the linear slope of eqs. (1) or (2),  $[\eta]$  could be obtained, which represented the intrinsic viscosity.

According to the additivity law, the  $[\eta]_{cal}$  was the calculated viscosity of the polymer system and it was got from Eq. (5):

$$[\eta]_{cal} = w_1[\eta]_{PVC} + w_2[\eta]_{PAN} \quad (5)$$

$[\eta]_{PVC}$  and  $[\eta]_{PAN}$  were the viscosity of PVC and PAN solution, which were got by Viscosity measurement. The mass fractions of PVC and PAN in the blend solutions are denoted by  $w_1$  and  $w_2$ , respectively:

$$\Delta[\eta] = [\eta]_{exp} - [\eta]_{cal} \quad (6)$$

Then,  $\Delta[\eta]$  was obtained from Eq. (6), which was the difference between the calculated viscosity value ( $[\eta]_{cal}$ ) and experimental value ( $[\eta]_{exp}$ ).

### FTIR spectroscopy analysis

FTIR spectroscopic measurements were carried out on a Bruker TEN-SOR37 spectrophotometer (Germany). There were 32 scans signal-averaged at a resolution of 4 cm<sup>-1</sup> from 4000 to 600 cm<sup>-1</sup>.

### DMA

The DMA curves of the membranes were obtained by a Netzsch DMA242 (Germany). The temperature range covered in this analysis was -50 to 150°C at a heating rate of 5°C/min, and the stress frequency was 1.5 Hz.

### SEM

The morphology of the membranes was observed with a FEI Quanta 200 scanning electron microscope (The Netherlands). The samples were broken during dipping in liquid nitrogen and sputtered with gold to maintain the cross-sectional structure of the membranes.

### Pure water flux (PWF)

PWF of the membranes was measured with hollow-fiber modules at 0.1 MPa of pressure and with a constant feed at room temperature. Time was first recorded after 15 min of running. PWF was calculated by Eq. (7):

$$J = \frac{V}{S \times t} \quad (7)$$

where  $J$  is the permeation flux of the membrane [L m<sup>-2</sup> h<sup>-1</sup> (0.1 MPa)],  $V$  is the quantity of the permeate

(L), and  $S$  is the membrane area ( $m^2$ ). Five samples were measured, and their average result is reported.

#### Porosity determination

The porosity ( $\varepsilon$ ) of the sample was calculated according to Eq. (8):

$$\varepsilon(\%) = \frac{(G_1 - G_2)/D_1}{(G_1 - G_2)/D_1 + G_2/D_2} \times 100\% \quad (8)$$

where  $G_1$  is the weight of the wet membrane,  $G_2$  is the weight of wet membrane,  $D_1$  is the water density ( $D_1 = 0.9908 \text{ g/cm}^3$ ), and  $D_2$  is the density of the blend membrane.

#### Mechanical performance

The mechanical performance of the PVC/PAN blend hollow-fiber membrane was tested by an electronic single-yarn strength tester PC-YG061 (Laizhou, China). The length of the membrane sample and the tensile rate were 250 mm and 250 mm/min, respectively. Readings for each specimen were taken to evaluate the average value.

## RESULTS AND DISCUSSION

### Compatibility study of PVC with PAN

Miscibility based on the thermodynamic compatibility

The solubility parameter is one of most common criteria used to adjudge the compatibility of blend polymer systems.<sup>4,19,20</sup> Hansen found that molecular interaction was composed of dispersive interaction, dipolar interaction, and hydrogen bonding. Therefore, the respective solubility parameters ( $\delta_d$ ,  $\delta_p$ , and  $\delta_h$ ) could be expressed by Eq. (9):

$$\delta^2 = \delta_d^2 + \delta_p^2 + \delta_h^2 \quad (9)$$

Hildebrand thought that the thermodynamic compatibility among polymers could be represented by the solubility parameter ( $\delta$ ), and it is given as the entropy of mixing ( $\Delta H_m$ ) by Eq. (10):

$$\Delta H_m = \phi_1 \phi_2 [(\delta_{d1} - \delta_{d2})^2 + (\delta_{p1} - \delta_{p2})^2 + (\delta_{h1} - \delta_{h2})^2] \quad (10)$$

where  $\phi$  is the volume fraction of the blend component and the subscripts 1 and 2 refer to the two polymers.

On the basis of solution theory, the compatibility of two polymers is mainly determined by  $\Delta H_m$ . The lower the value of  $\Delta H_m$  is, the better the compatibility of the two polymers will be. The solution param-

**TABLE I**  
Solubility Parameters of the PVC and PAN Polymers and the Solvent DMAc

Substance	$\delta_d$ (MPa) <sup>1/2</sup>	$\delta_p$ (MPa) <sup>1/2</sup>	$\delta_h$ (MPa) <sup>1/2</sup>	$\delta$ (MPa) <sup>1/2</sup>
$\delta_{PVC}$	18.7	10	3.1	21.43
$\delta_{PAN}$	16.47	23.25	7.27	29.41
$\delta_{DMAc}$	16.8	11.5	10.2	22.7
$ \delta_{PVC} - \delta_{PAN} $	2.37	13.25	4.17	7.98
$ \delta_{PVC} - \delta_{DMAc} $	1.9	1.5	7.1	1.33
$ \delta_{PAN} - \delta_{DMAc} $	0.47	11.75	3.07	4.71

eter difference between PVC and PAN, shown in Table I, was obtained, and the  $\Delta H_m$  value of the PVC/PAN blend system is higher. Therefore, it could be seen that PVC and PAN were partly incompatible. However, analyzing the structure of PVC and PAN, we found that both PVC and PAN were polar polymers; one had two  $-Cl$  groups, and the other contained a strong polar  $C \equiv N$  group. With the provision that a proper solvent is chosen, they should be miscible at some composition and temperature. DMAc is a polar nonproton solvent and a proper one for the polar polymer and mixed these two blend polymers together well. When the phase separation occurred, the system was unstable, and IFMs were formed because of the far difference between  $\delta_1$  and  $\delta_2$  of the two polymers.

#### Viscosity method

The viscosity study of the compatibility of the blend polymer is an attractive method because of its simplicity and effectiveness. The blend solutions of PVC and PAN were prepared in DMAc at 30°C with different contents of PAN (0, 10, 20, 30, 70, 80, 90, and 100). It has been reported that attractive interaction between the chains of two different polymers in solution may result in an expansion of the polymer coils and an increase in the intrinsic viscosity. The intrinsic viscosity ( $[\eta]$ ) represents the effective hydrodynamic volume of a polymer molecule in solution.

Figure 1 shows the plots of the reduced intrinsic viscosity ( $\eta_{sp}/c$ ) versus  $c$  for the PVC/PAN blends in DMAc solution at 30°C. All of the plots were linear in the whole range of  $c$ . On extrapolation to zero  $c$ , the intrinsic viscosity of the PVC/PAN blend solution in DMAc was obtained. It is noted that the intrinsic viscosity of PVC in DMAc solution was variable with the addition of PAN. Figure 2 shows the  $\Delta[\eta]$  values for the PVC/PAN blend solution with various PAN amounts in DMAc at 30°C. This showed that the  $\Delta[\eta]$  values of the PVC/PAN blends were not equal to zero. Negative deviation was demonstrated at  $W_2 \geq 20\%$  and  $W_2 \leq 80\%$ ; this reflected the expansion of both the PAN and PVC

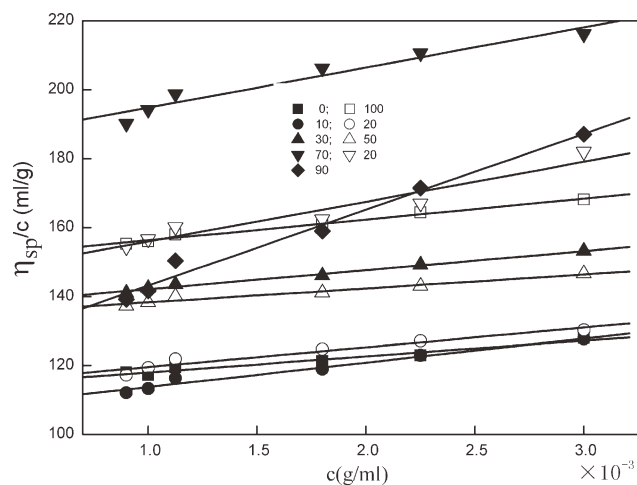


**Figure 1** Plots of  $\eta_{sp}/c$  versus  $c$  for the PVC/PAN blends in DMAc solution at 30°C.

coil dimensions due to strong intermolecular interaction or compatibility between them, and positive deviation was displayed in the region of  $W_2$  from 20 to 80%. This meant that the shrinking of both PAN and PVC coil dimensions occurred because of incompatibility between them. The regions of compatibility at both sides were probably dependent on higher  $c$  values of functional groups of chloride or nitrile in the blends.

#### FTIR spectroscopy

FTIR spectroscopy has been proven to be a useful technique for detecting the characterization of specific intermolecular interactions between the groups in different polymer molecules and conformational changes occurring in compatible blend systems. Figure 3 shows the FTIR spectra of the pure PVC, PAN, and PVC/PAN blend membranes.

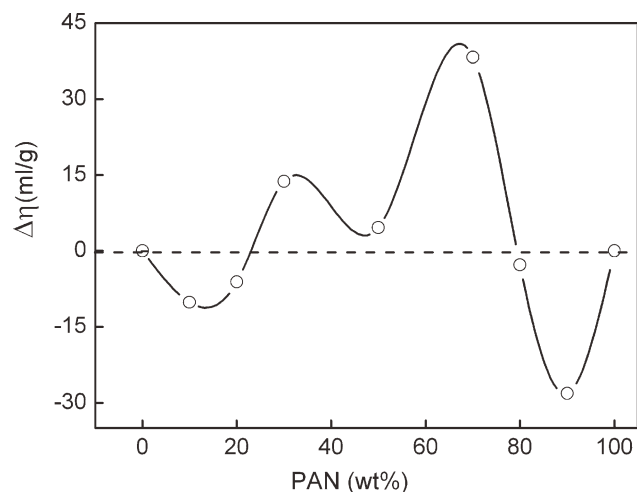


**Figure 2** Variation of  $\Delta[\eta]$  with  $W_{PAN}$  in the PVC/PAN blend.

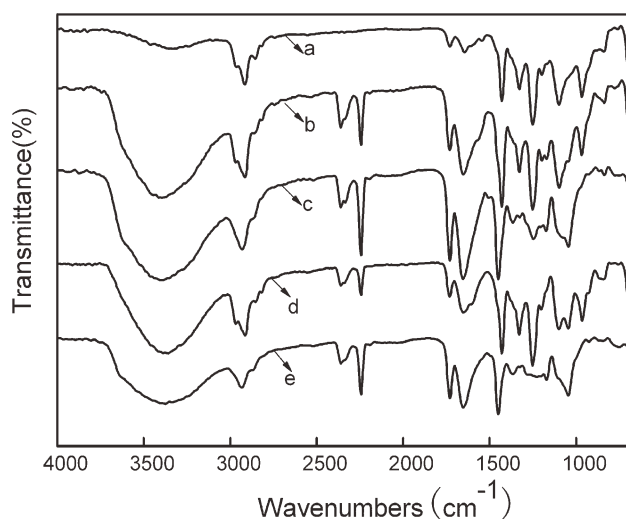


**Figure 3** FTIR plot of (a) PVC, (b) PVC/PAN (90/10), (c) PVC/PAN (70/30), (d) PVC/PAN (10/90), and (e) PAN.

The FTIR spectrum of pure PVC was characterized by strong absorption peaks at 1430, 1330, and 1250  $\text{cm}^{-1}$ , which were attributed to  $\text{CH}_2$  deformation vibration bands and CH stretching vibrations [Fig. 3(a)]. The peaks at 1099 and 966  $\text{cm}^{-1}$  were due to the in-plane and out-of-plane CH bending modes, and the band at 692  $\text{cm}^{-1}$  in pure PVC [Fig. 3(a)] was assigned to C—Cl stretching vibrations. The spectrum of PAN had a very strong absorption peak at 2245  $\text{cm}^{-1}$ , which was attributed to  $\text{C}\equiv\text{N}$  stretching vibrations [Fig. 3(e)]. The absorbencies at 2941 and 2943  $\text{cm}^{-1}$  resulted from the asymmetric stretching vibration of  $\text{CH}_2$ , and the peaks at 1730 and 1654  $\text{cm}^{-1}$  were assigned to the second and third monomer by stretching vibrations of  $\text{C}=\text{O}$  and  $\text{C}=\text{C}$ . To a certain extent, this may have partly improved the hydrophilicity of the PVC membrane. Compared with the PVC membrane, there were new appearances of wide bands over the 2244–2245, 1730, and 1654- $\text{cm}^{-1}$  range in the PVC/PAN blend membrane; these resulted from the stretching vibrations of  $\text{C}\equiv\text{N}$ ,  $\text{C}=\text{O}$ , and  $\text{C}=\text{C}$ , respectively [Fig. 3(b–d)]. The spectrum of the blend membranes had hardly any shift compared with the spectrum of the two individual components; thus, the interaction between PVC and PAN was weak. Then, interface microvoids may have been produced during the phase separation in the PVC/PAN blend process.

#### DMA

The measurement of the glass-transition temperature ( $T_g$ ) of a polymer blend is often used as a criterion for determining its compatibility. A miscible polymer exhibited a single  $T_g$  between two components. With increasing miscibility of a blend polymer, there is a broadening of the transition, whereas incompatible blend systems would be marked by separate

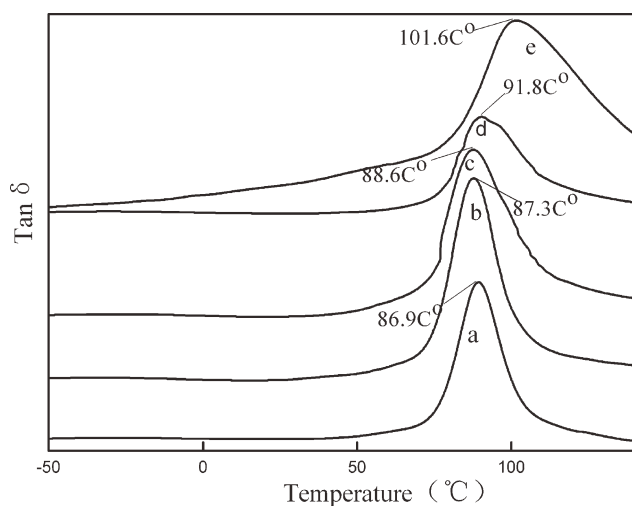


**Figure 4** DMA plot of (a) PVC, (b) PVC/PAN (90/10), (c) PVC/PAN (70/30), (d) PVC/PAN (10/90), and (e) PAN.

transitions of the polymer component in the blends. In DMA curves,  $T_g$  can be denoted by the  $x$  coordinate of the tangent peak. To ascertain the miscibility of the PVC/PAN blend,  $T_g$  was measured by DMA in Figure 4. It can be seen from Figure 4 that  $T_g$  of the PVC/PAN blend membranes was higher than that of pure PVC and lower than that of PAN. There are several classical equations that correlate  $T_g$  of a blend miscible system with its composition. These equations

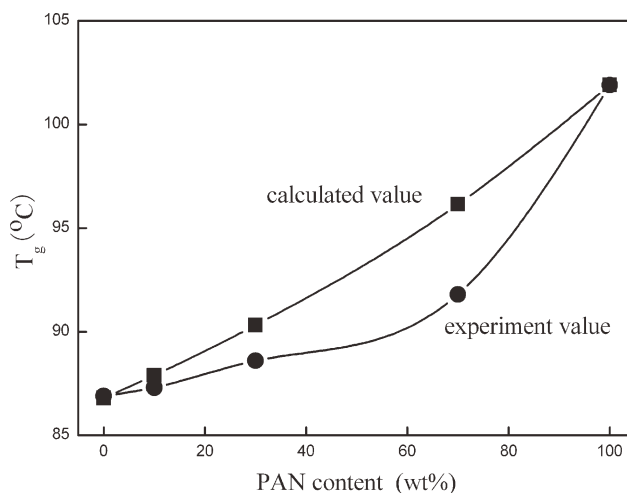


**Figure 5** Effect of the content of PVC/PAN on  $T_g$ .

were used to interpret both positive and negative deviations from the role of the mixtures and the S-shaped  $T_g$  versus blend composition curves. Figure 5 shows the curve predicted from the  $T_g$  composition, which was obtained from the Fox equation [Eq. (11)]:

$$1/T_g = w_1/T_{g1} + w_2/T_{g2} \quad (11)$$

where  $T_g$ ,  $T_{g1}$ , and  $T_{g2}$  are the glass-transition temperatures of the blend membrane, PVC membrane,

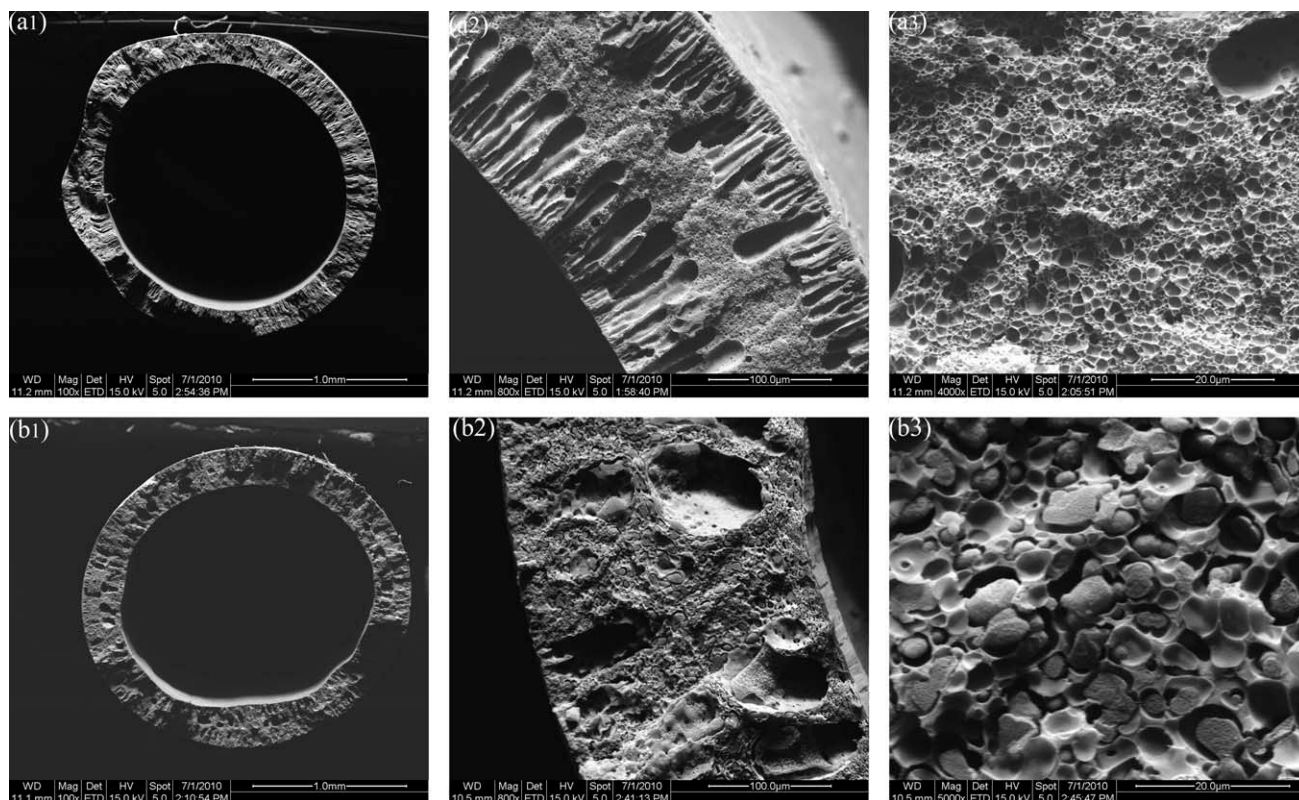


**Figure 6** SEM photographs of the cross sections of the (a) PVC membrane and (b) PVC/PAN (70/30) blend membrane: (1) 100, (2) 600, and (3) 5000 $\times$ .

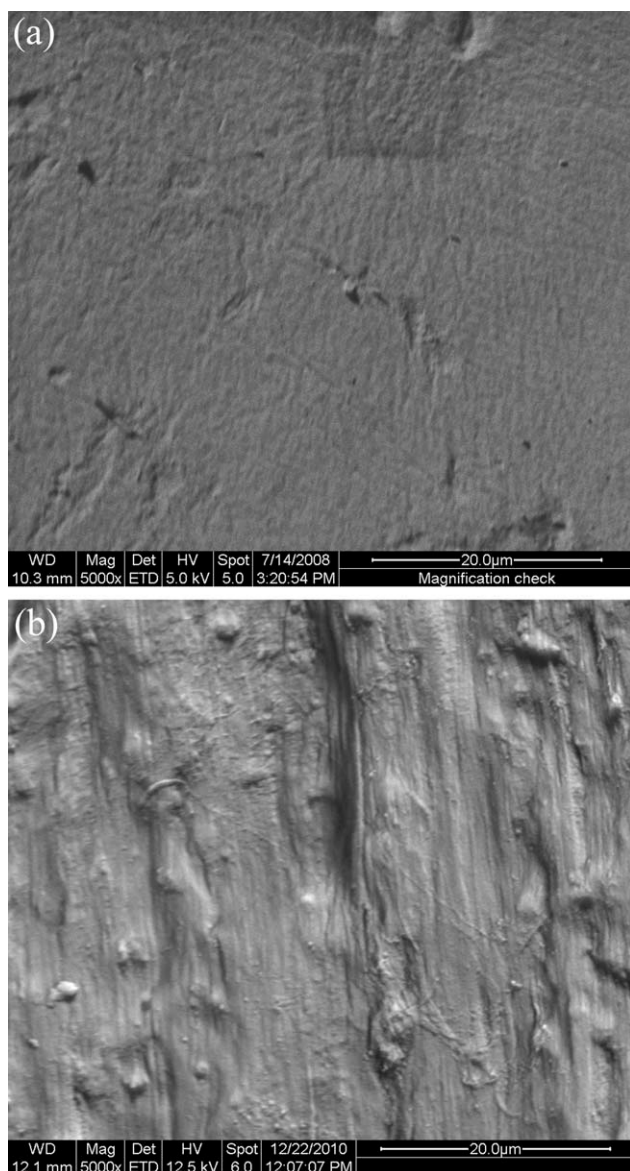


**Figure 7** Outer surface of the (a) PVC membrane and (b) PVC/PAN (70/30) blend membrane.

and PAN membrane, respectively.  $T_g$  of the blend membrane from the calculated equation turned out to have a similar negative deviation in the region of  $W_2$  from 20 to 80%; however,  $T_g$  of membrane was much different between the experimental value and the calculated one, from which we obtained many more interfacial macrovoids during the phase separation.

#### Morphology of the PVC/PAN blend hollow-fiber membrane

The morphologies of PVC and the PVC/PAN blend hollow-fiber membranes are depicted in Figure 6. As can be seen, the cross-sectional structures of all of the membranes were similar. Near the out and inner

walls, fingerlike pores were obtained, and sponge-like structures were present in the middle of the membranes. Figure 6(a) shows that the pores in the PVC membrane had two-layer fingerlike structures going through the middle-side membrane to the end side of the membrane and sponge-like structures in the middle of the cross section. Because pure water was used as both the inner and outer precipitants, asymmetric membrane structures could be easily formed. In a comparison made between the morphologies of the PVC and PVC/PAN blend membranes, the cross section of the PVC/PAN blend membrane consisted of large voids in the shape of spheres or ellipsoids, and there was a transparent IFM structure between these voids. In Figure 6(b), the cross-sectional structure of the PVC/PAN blend

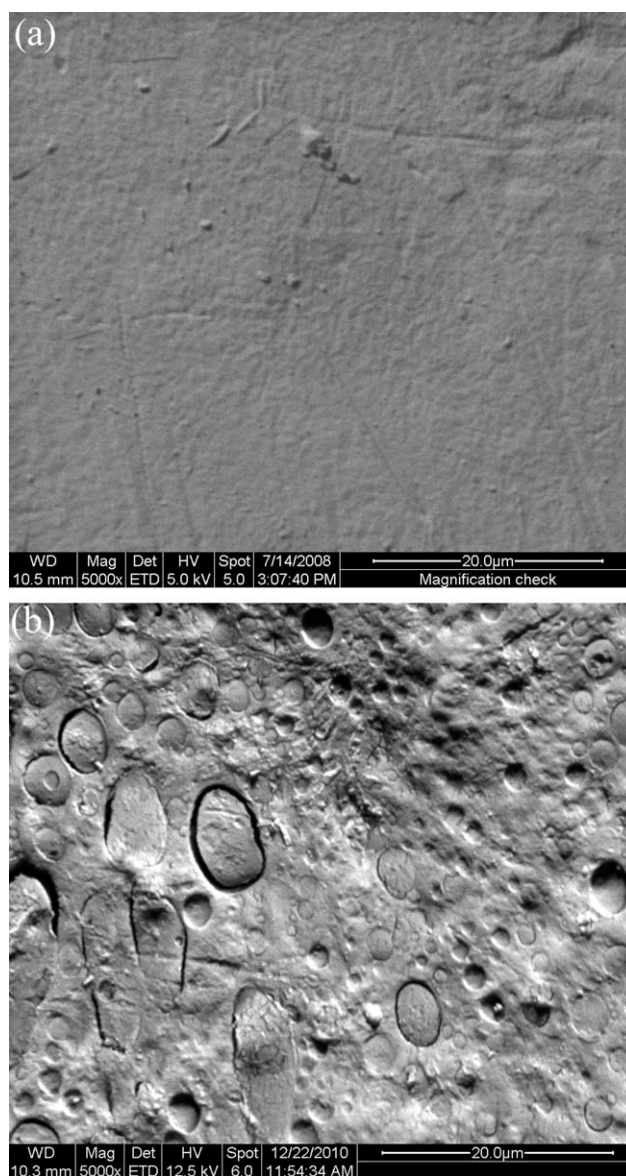


**Figure 8** Inner surface of the (a) PVC membrane and (b) PVC/PAN (70/30) blend membrane.

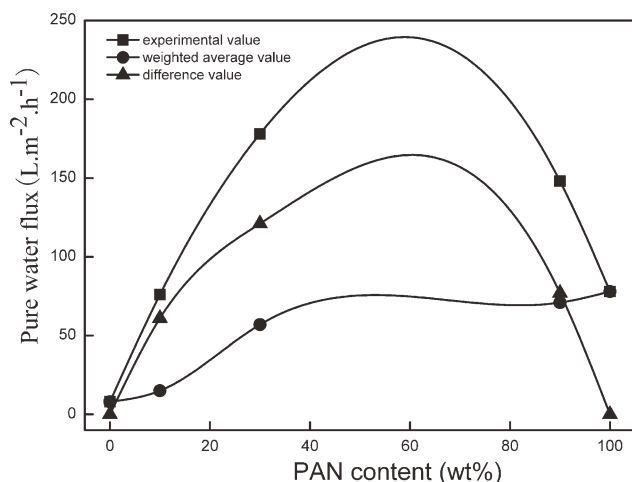


**Figure 9** Measurement of PWF of the PVC/PAN blend membrane.

membrane prepared with  $W_{\text{PAN}} = 30\%$  in the dope solution looks more like IFMs, and the shape of the spheres or ellipsoids is smaller. The experimental results illustrate that the precipitation of the PVC/PAN blend forming the membrane structure and the exchange of solvents with nonsolvent (water) may have been affected by the diffusion of the compatibility between PVC and PAN from the dope solution to the water bath. All of these results were very consistent with the thermodynamic analysis and experiments. Figures 7 and 8 show the results of the outer and inner surfaces of the PVC hollow-fiber membrane and PVC/PAN blend hollow-fiber membrane, respectively. As shown, compared with the PVC membrane, the PVC/PAN blend membrane had a rougher surface with obvious interfacial macrovoids. This phenomenon may have been due to the incompatibility between PVC and PAN when phase separation occurred.

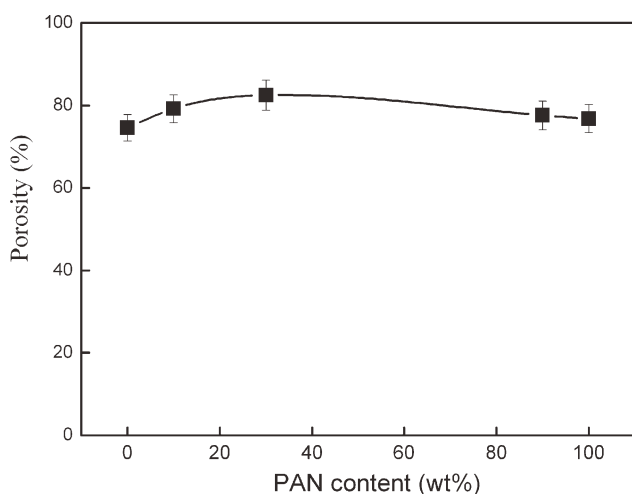


**Figure 10** Porosity of the PVC/PAN blend membrane.

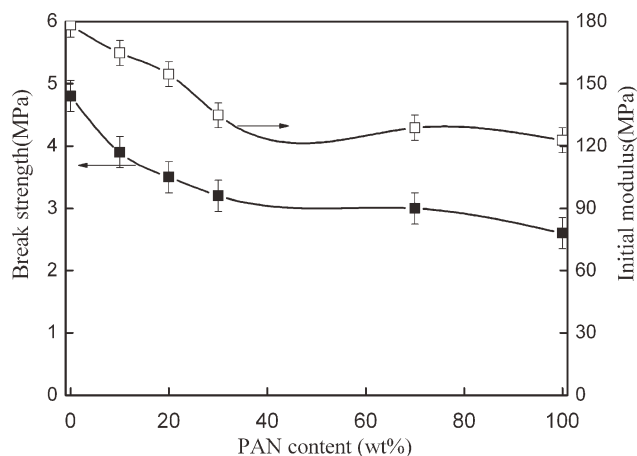


**Figure 11** Measurement of the mechanical performance of the PVC/PAN blend membrane.

### Effect of the IFMs on the permeation of the blend membrane

The permeation characteristics of the PVC, PAN, and PVC/PAN blend membranes, such as PWF and porosity, are described in Figures 9 and 10. As shown, the PWF and porosity of the PVC membrane were a little lower than that of the PAN membrane, and the values of the PVC/PAN blend membrane were greater than that of the PVC or PAN pure membrane. This may be attributed to the fact that the hydrophile of PAN was better than PVC. Another reason for the increasing effect PAN may have been the formation more IFMs to enhance the porous of blend membrane. To describe the effect of IFMs on the PVC/PAN blend membrane, we cite the weighted average equation and difference value, which are defined by  $F = W_1F_1 + W_2F_2$ , where  $F$ ,  $F_1$ , and  $F_2$  are the PWFs of the weight average of the PVC/PAN blend membrane, the pure PVC membrane, and the pure PAN membrane, respectively. The weighted average and difference value curves are shown in Figure 9. Obviously, the experimental values were all much higher than those of the two pure membranes and also those of the weighted averages. It is shown that the difference value, which proved the IFMs attributed much to the PWF of the blend membrane with an increase in the PAN content of the polymer  $c$ , turned to the better with the  $W_1/W_2$  equal to 70/30. The PVC/PAN blend membranes showed a greater porosity, as shown in Figure 10. With an increase in the content of PAN in the blend dope solution, the polymer chains and the higher viscosity of the blend polymer solution prohibited the exchange of the solvent with more IFM deformation through the phase-separated polymer solution. The membrane morphologies in Figure 6 could also explain these experimental results.

### Effect of the IFMs on the mechanical properties of blend membrane

To evaluate the mechanical properties of the PVC/PAN blend membrane in industrial applications, the values of the tensile strength and initial strength of blend membranes were determined. Figure 11 shows the mechanical properties of the PVC/PAN blend membrane. It could be seen that both the tensile strength and initial strength of the blend membrane decreased slightly with increasing PAN content in the blend dope solution. This suggests that the mechanical properties of the PVC/PAN blend membrane were mainly approximately determined by the permeation of the blend membrane, which generated a looser surface with many more IFMs in the blend membrane.

### CONCLUSIONS

On the basis of the compatibility of the blend polymer, it was possible to produce a PVC/PAN blend hollow-fiber membrane with a new porous structure-IFMs. The compatibility results of this PVC/PAN system indicate that PVC and PAN were incompatible; therefore, IFMs were produced as a result of phase separation. The PWF and porosity of the PVC/PAN blend membrane were much greater than the those of pure polymer membrane with the IFMs' existence. Compared to those of the PVC membrane, the break strength and initial strength of the PVC/PAN blend membrane decreased slightly; this suggested that the blend membrane may have had a looser structure. We will investigate whether PAN can also improve the antifouling property of

PVC/PAN blend hollow-fiber membranes after hydrolysis in the future.

### References

1. Zhao, Y.; Qian, Y.; Zhu, B.; Xu, Y. *J Membr Sci* 2008, 310, 567.
2. Xiuli, Y.; Hongbin, C.; Xiu, W.; Yongxin, Y. *J Membr Sci* 1998, 146, 179.
3. Wang, D.; Li, K.; Teo, W. K. *J Membr Sci* 2000, 178, 13.
4. Li, N.; Xiao, C.; An, S.; Hu, X. *Desalination* 2010, 250, 530.
5. Xiaoyu, H.; Changfa, X.; Shulin, A.; Guangxia, J. *J Mater Sci* 2007, 42, 6234.
6. Xiao, C. F.; Zhang, Y. F.; Wu, S. Z.; Takahashi, T. *J Appl Polym Sci* 2002, 83, 394.
7. Xu, J.; Xu, Z. *J Membr Sci* 2002, 208, 203.
8. An, Q. F.; Qian, J. W.; Sun, H. B.; Wang, L. N.; Zhang, L.; Chen, H. L. *J Membr Sci* 2003, 222, 113.
9. Peng, Y.; Sui, Y. *Desalination* 2006, 196, 13.
10. Ulutan, S.; Balke, D. *J Membr Sci* 1996, 115, 217.
11. Rajendran, S.; Babu, R. S.; Sivakumar, P. *J Membr Sci* 2008, 315, 67.
12. Hosseini, S. M.; Madaeni, S. S.; Khodabakhshi, A. R.; Zendehtnam, A. *J Membr Sci* 2010, 365, 438.
13. Bureau, E.; Cabot, C.; Marais, S.; Saiter, J. M. *Eur Polym J* 2005, 41, 1152.
14. Mano, V.; Felisberti, M. I.; Matencio, T.; De Paoli, M. *Polymer* 1996, 37, 5165.
15. Marais, S.; Bureau, E.; Gouanv, F.; Ben Salem, E.; Hirata, Y.; Andrio, A.; Cabot, C.; Atmani, H. *Polym Test* 2004, 23, 475.
16. Yang, M.; Liu, T. *J Membr Sci* 2003, 226, 119.
17. Gopalan, A. I.; Santhosh, P.; Manesh, K. M.; Nho, J. H.; Kim, S. H.; Hwang, C.; Lee, K. *J Membr Sci* 2008, 325, 683.
18. Qin, J.; Cao, Y.; Li, Y.; Li, Y.; Oo, M.; Lee, H. *Sep Purif Technol* 2004, 36, 149.
19. Bridge, M. J.; Broadhead, K. W.; Hlady, V.; Tresco, P. A. *J Membr Sci* 2002, 195, 51.
20. Kim, J. H.; Min, B. R.; Won, J.; Park, H. C.; Kang, Y. S. *J Membr Sci* 2001, 187, 47.